

ARMY RESEARCH LABORATORY



**Three-Dimensional Change Detection
With the Use of an Evidence Grid**

by Gary A. Haas

ARL-TR-3916

September 2006

NOTICES

Disclaimers

The findings in this report are not to be construed as an official Department of the Army position unless so designated by other authorized documents.

Citation of manufacturer's or trade names does not constitute an official endorsement or approval of the use thereof.

DESTRUCTION NOTICE—Destroy this report when it is no longer needed. Do not return it to the originator.

Army Research Laboratory

Aberdeen Proving Ground, MD 21005-5066

ARL-TR-3916

September 2006

Three-Dimensional Change Detection With the Use of an Evidence Grid

Gary A. Haas

Weapons and Materials Research Directorate, ARL

REPORT DOCUMENTATION PAGE

Form Approved
OMB No. 0704-0188

Public reporting burden for this collection of information is estimated to average 1 hour per response, including the time for reviewing instructions, searching existing data sources, gathering and maintaining the data needed, and completing and reviewing the collection information. Send comments regarding this burden estimate or any other aspect of this collection of information, including suggestions for reducing the burden, to Department of Defense, Washington Headquarters Services, Directorate for Information Operations and Reports (0704-0188), 1215 Jefferson Davis Highway, Suite 1204, Arlington, VA 22202-4302. Respondents should be aware that notwithstanding any other provision of law, no person shall be subject to any penalty for failing to comply with a collection of information if it does not display a currently valid OMB control number.

PLEASE DO NOT RETURN YOUR FORM TO THE ABOVE ADDRESS.

1. REPORT DATE (DD-MM-YYYY) September 2006		2. REPORT TYPE Final		3. DATES COVERED (From - To) 2006	
4. TITLE AND SUBTITLE Three-Dimensional Change Detection With the Use of an Evidence Grid				5a. CONTRACT NUMBER	
				5b. GRANT NUMBER	
				5c. PROGRAM ELEMENT NUMBER	
6. AUTHOR(S) Gary A. Haas (ARL)				5d. PROJECT NUMBER AH03	
				5e. TASK NUMBER	
				5f. WORK UNIT NUMBER	
7. PERFORMING ORGANIZATION NAME(S) AND ADDRESS(ES) U.S. Army Research Laboratory Weapons and Materials Research Directorate Aberdeen Proving Ground, MD 21005-5066				8. PERFORMING ORGANIZATION REPORT NUMBER ARL-TR-3916	
9. SPONSORING/MONITORING AGENCY NAME(S) AND ADDRESS(ES)				10. SPONSOR/MONITOR'S ACRONYM(S)	
				11. SPONSOR/MONITOR'S REPORT NUMBER(S)	
12. DISTRIBUTION/AVAILABILITY STATEMENT Approved for public release; distribution is unlimited.					
13. SUPPLEMENTARY NOTES					
14. ABSTRACT In this study, the objective is to find changes in terrain geometry, which are encountered by a patrolling unmanned ground vehicle (UGV) from one patrol run to another. The UGV is equipped with a streaming imaging ladar (laser radar) that measures the distance to the nearest surface at an array of points spanning a prism-shaped field of view and with a navigation system that measures the location of the UGV in a world-fixed coordinate frame. The path followed by the UGV is approximately the same during each run. We are interested in the ability to detect true changes, to reject false alarms, and the range relative to the UGV at which detections occur.					
15. SUBJECT TERMS change detection; ladar; UGV					
16. SECURITY CLASSIFICATION OF:			17. LIMITATION OF ABSTRACT SAR	18. NUMBER OF PAGES 25	19a. NAME OF RESPONSIBLE PERSON Gary A. Haas
a. REPORT Unclassified	b. ABSTRACT Unclassified	c. THIS PAGE Unclassified			19b. TELEPHONE NUMBER (Include area code) 410-278-8867

Contents

List of Figures	v
List of Tables	v
1. Background	1
2. Problem Statement	1
2.1 Imaging Ladar Technology	1
2.2 Spatial Resolution and Voxels	3
2.3 Evidence Grid.....	3
2.4 Change Detection	4
3. Approach	4
4. Method	6
5. Results	6
5.1 FITG 143-144.....	7
5.2 FITG 129-130.....	8
5.3 FITG 129-131.....	8
6. Discussion	10
6.1 Distribution of Voxelized Data	10
6.2 Vantage Point	11
6.3 Occlusion.....	11
6.4 Surface Versus Volume.....	11
6.5 Range Effects	11
6.6 Path Dependence	11
6.7 Registration	12
6.8 Distribution of the Difference in Voxel Content.....	12
7. Conclusions	13

8. References	14
Distribution List	18

List of Figures

Figure 1. Scanning imaging lidar.	2
Figure 2. Left figure is a single scan of intersection of two walls at ~15 m; right figure shows several hundred scans of a human in woods at ~15 m, colored by elevation.	3
Figure 3. Cumulative distribution of p_1 for patrol 143.	10
Figure 4. Cumulative distribution of diff between patrol 143 and 144	12
Figure A-1. Objective: Find change from patrol to patrol.	15
Figure A-2. Ladar return interpreted as line segment.	15
Figure A-3. Space interpreted as voxels.	15
Figure A-4. Tracing a “ray”.	15
Figure A-5. Probability that a voxel is occupied, $P(\text{occ})$	16
Figure A-6. Voxel state at end of first patrol	16
Figure A-7. Ready for second patrol.....	16
Figure A-8. Begin second patrol.....	16
Figure A-9. Find $P(\text{occ})$ for each voxel during second patrol	17
Figure A-10. Compare $P(\text{occ})$ for the two patrols	17
Figure A-11. Find change voxels.....	17
Figure A-12. Find change regions	17

List of Tables

Table 1. The attributes of a voxel.	5
--	---

INTENTIONALLY LEFT BLANK.

1. Background

An unmanned ground vehicle (UGV) capable of autonomous mobility is typically equipped with a navigation system for sensing the UGV's position in the world and a sensor for detecting obstacles. An obstacle-detecting sensor based on ladar (often interpreted as a portmanteau of *laser radar* and used interchangeably with *lidar*) is frequently used. Returns from the ladar sensor classify points of the terrain as "occupied" (presumably ground or an obstacle); volumes from which no returns are received are "free space" or unknown. This sensor information enables the construction of a model of the world (the *world map*) used by the UGV to plan its route to the goal location, driving on terrain known to be "ground" (occupied and horizontal) and avoiding obstacles detected in its path. A world map is frequently discretized at a resolution suitable for navigation, and the presence or absence of ladar returns is abstracted to indicate the binary state of the nearby enclosing volume. The resulting world map may be no more than a two-dimensional (2-D) grid classifying each grid square as "passable" or "obstacle," or a (so-called) two-and-a-half dimensional grid representing the elevation of the grid square.

2. Problem Statement

In this study, the UGV obstacle-detecting sensor is used to construct a full three-dimensional (3-D), although simplified, world model during a UGV patrol through an area. Then, in a second patrol through the same terrain, the UGV contrasts fresh sensor data against the world model created during the first patrol to judge what elements of the terrain have changed from free space to occupied space or vice versa. It is assumed that the terrain is static during each patrol and that the only changes of interest occur between patrols. It is recognized that these assumptions are unlikely to hold in any kind of realistic scenario. The study is intended as a precursor to a method for recognizing a moving obstacle, particularly a moving pedestrian, during a patrol with the use of the sensors native to an autonomous UGV.

2.1 Imaging Ladar Technology

The ladar sensor is favored by the UGV community since it implicitly senses the range from the UGV to an obstacle in a specific direction (unlike a video sensor which senses the color in a specific direction, or a sonar sensor which senses the range in a general direction). Ladar works on the principle of "time of flight" of a laser pulse to something in its path, which can readily be converted to a distance or range. By combining the range and direction information from the ladar sensor with the UGV position from the navigation system, one can build a map of the world in a time-invariant coordinate system that allows sensor information to be accumulated

and integrated over time. The detailed phenomenology of lidar sensing is beyond the scope of this report.

The imaging lidar used in this study collects data, not as a single time-of-flight measurement but in a temporal stream of such measurements. Facets of a spinning mirrored prism sweep a bank of pulsed laser beams across the terrain, as in figure 1. Each facet reflects the beam at a characteristic angle (A) with respect to axis of spin and traces a partial conic surface through space. A laser pulse synchronized with rotational displacement (T) of the mirror results in a reflected return which is sensed. The time of flight between pulse and return is converted to a distance that corresponds to the *range* (D) to a point on the cone. This range measurement in the context of its direction in A and T is termed a “*rangel*” (from *range pixel*). Geometry converts the point at D, T, A to a point at Cartesian X, Y, Z in sensor coordinate frame. A *scan* is the set of all such points from all facets as the spinning prism completes one rotation.¹ Each point measured is effectively the output of a line-of-sight sensor. The scan thus samples a surface bounding the line of sight from the sensor to the surrounding terrain.

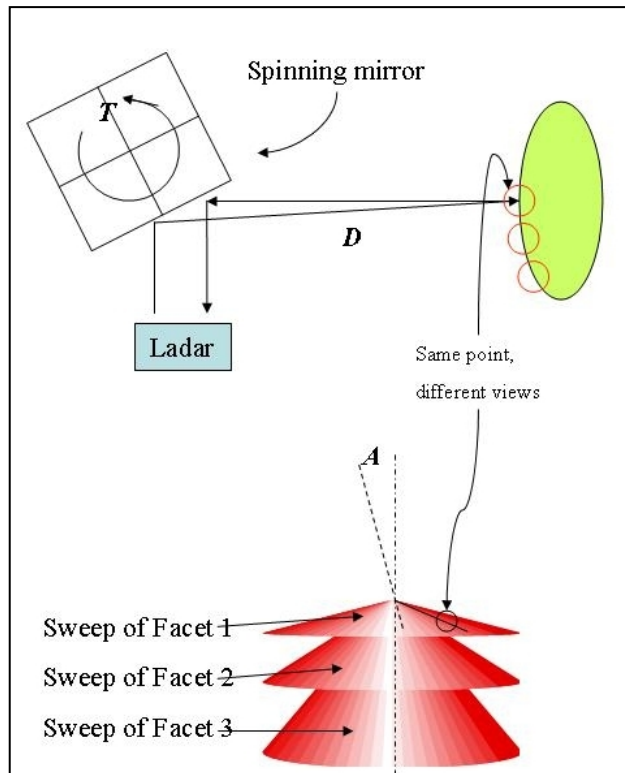


Figure 1. Scanning imaging lidar.

¹If the facets are designed so that the swept volumes align and adjoin, a scan so created can be represented as a *range image*, a pixel-like matrix of range values mapping successive values of A and T into indices of image row and column. This can be useful for visualization by assigning false color to the range value D . However, the “rows” swept by pulses reflected from a facet are not lines but arcs, so an image constructed along linear rows and columns, as is conventional, appears distorted.

A single scan from this lidar is of limited resolution, but scans occur at a rate comparable to video frame rate. When mounted on a moving vehicle, the lidar senses the terrain frequently and from vantage points that change as the vehicle progresses along its path, effectively sampling the terrain at a spatial frequency higher than the raw sensor resolution would indicate. Sensor data from a stream of scans can be combined with sensed vehicle location information from the UGV's navigation system and converted to a common (world) coordinate system, allowing the aggregation of terrain information. The aggregated sensor information is dense but distributed in an irregular fashion across the terrain. An example of the effect of this aggregation is shown in figure 2.

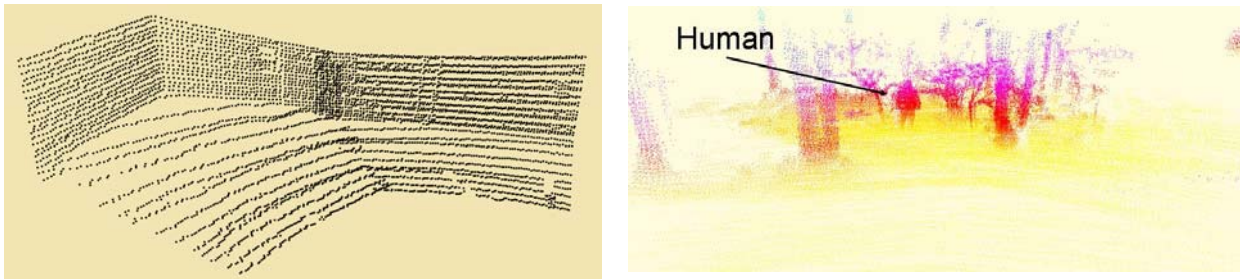


Figure 2. Left figure is a single scan of intersection of two walls at ~15 m; right figure shows several hundred scans of a human in woods at ~15 m, colored by elevation.

Data for this study were generated by an imaging lidar built by General Dynamics Robotic Systems (GDRS). The GDRS lidar has been described in Shneier et al. (2003). Other imaging lidar technologies exist; several are described in Juberts and Barbera (2004).

2.2 Spatial Resolution and Voxels

In practical applications of terrain change detection, there is a lower limit to the magnitude of change, which is of interest. This limit is dictated by the application and precision of the sensor. In this study, we are uninterested in any change smaller than the smallest dimension of a human torso (roughly 0.2 meter), and the precision of the sensor is believed to be several centimeters. Therefore, we can simplify the problem and reduce the amount of data to be accumulated by mapping the data into a grid with resolution appropriate to the application. In this case, we define a 3-D matrix on 0.1-meter centers. This grid is said to be made of *voxels*, “a portmanteau of the words *volumetric* and *pixel*”². Its resolution was chosen to avoid the aliasing that results from sampling at a interval greater than the (spatial analog of) Nyquist “rate” and is believed to be approximately the correct size for this study.

2.3 Evidence Grid

As observed previously, the sensor samples the terrain in an irregular pattern governed by the path traversed by the sensor. Comparison of two patrols on a point-by-point basis is thus not

²<http://en.wikipedia.org/wiki/Voxel>

possible, and even comparison on a voxel-by-voxel basis requires some sort of normalization to compensate for differences in the actual sampling realized. One method that has proved useful in similar problems is the *evidence grid*. In this scheme, grid cells are not simply classified as occupied or unoccupied but instead store the evidence (certainty) that the cell is occupied or empty. Martin and Moravec (1996) describe several variants of evidence grids and an underlying framework grounded in probability theory. The approach of this study is similar to an early version of Moravec's work, without theoretical framework. It is described in detail in section 3.

2.4 Change Detection

Change detection in 3-D sensor data has infrequently been reported to have been applied to UGV sensor data. An exception (without details) is Pacis et al. (2005). Schutz and Hugli (1996) described change detection in toy scenes using data from an optical striper. Processing occurred in the range image domain rather than the 3-D domain, and the focus was occlusion. Change detection techniques have been applied to elevation maps or classification maps constructed from 3-D ladar or synthetic aperture radar (SAR) (e.g., Tuong et al., 2004). Change detection in 3-D medical images is more common (e.g., Maintz and Viergever, 1998). Three-dimensional data from ladar and SAR are more typically applied to target acquisition problems, which are related but different (Bhanu et al., 1997).

In 2-D applications, typically based on video imagery, change detection is a common element in a host of applications, notably video surveillance and remote sensing. An excellent survey is presented in Radke et al. (2005).

3. Approach

The approach used in this study is based on a voxel-based world model. This representation enables volumes that correspond spatially to be compared between patrols. We endeavor to classify voxels as “changed” or “not changed,” based on a specified minimum change between patrols in the evidence of a voxel being occupied. Evidence of a voxel being occupied during a patrol is measured by the number of times it was discovered to be occupied, normalized by the number of times the voxel has been encountered. The process by which this classification occurs is described further. Presentation graphics illustrating the process are shown in appendix A. The following text tracks these figures and references figures as appropriate. The reader may find it helpful to read the two in tandem.

Sensor data from the first patrol is parsed so that each data point, in world XYZ coordinates, is paired with the spatial location of the sensor at the time of the sense. These are termed the *point* and the *viewpoint* of the data pair. Each pair thus defined a line segment, termed (following

conventions of the computer graphics community) a *ray*. This is depicted in figures A-1 and A-2.

The volume spanned by the sensor data from the first patrol is divided into cubic voxels at a resolution of 0.1 meter, as in figure A-3. Each voxel is assigned a set of attributes, defined in table 1. The attributes **occ**, **no_occ**, **p_occ**, and **diff** are dynamic and change as we collect more sensor information. The attribute **p_1** is aggregate and assumes a value only at the conclusion of processing sensor data from the first patrol. During processing of data from the first patrol, **p_1** and **diff** are undefined.

Table 1. The attributes of a voxel.

occ	The number of times a voxel was discovered to be occupied during this patrol
no_occ	The number of times a voxel was discovered to be empty during this patrol
p_occ	The probability that a voxel is occupied
p_1	The probability that a voxel was occupied during patrol 1
diff	The probability the voxel has changed since patrol 1

With a technique from computer graphics known as *ray tracing* (Amanatides and Woo, 1987), the voxels encountered by the ray are identified. The voxel corresponding to the terminal point of the ray increments its **occ** attribute, indicating an increase in evidence that the voxel is occupied. Any voxel completely traversed by the ray increments its **no_occ** attribute, indicating an increase in evidence that the voxel is free space and not occupied. This is depicted in figures A-4 and A-5.

When all data from the patrol are processed, the ratio **p_occ**, representing a measure of the evidence that the voxel is occupied based on current evidence accumulated, is calculated for each voxel, from

$$\mathbf{p_occ} = \mathbf{occ} / (\mathbf{occ} + \mathbf{no_occ})$$

With all evidence from the first patrol having been processed, each voxel's **p_occ** is assigned to its **p_1** attribute, representing the evidence that the voxel was occupied during the first patrol, as in figure A-6. At this point, processing of the first patrol is complete, and we begin processing data from the second patrol. Figure A-7 addresses the transition.

Data from the second patrol is loaded and parsed into rays; **occ** and **no_occ** attributes are cleared to initialize the processing of the second patrol. As in the processing of the first patrol, the rays from the second patrol are traced, **occ** and **no_occ** incremented for all affected voxels, figures A-8 and A-9.

To identify change voxels, the ratio **p_occ** is calculated for each voxel and compared to the corresponding **p_1**. The difference **diff** between the voxel **p_occ** at the time of the event and its **p_1** from the first patrol is calculated as

$$\mathbf{diff} = \mathbf{abs}(\mathbf{p_occ} - \mathbf{p_1})$$

and the **diff** values are thresholded to differentiate *change voxels* (voxels with **diff** > **v_threshold**) from *background voxels* (voxels with **diff** < **v_threshold**). This is depicted in figures A-10 and A-11.

To reduce outliers, change voxels are aggregated into *change regions*, as in figure A-12. Any change voxel within a distance threshold **r_threshold** of the centroid of an existing change region is assigned to the region, and the centroid is recomputed. In a cleanup step, overlapping pairs of change regions are absorbed by the larger of the pair.

4. Method

This study is intended to evaluate the effectiveness of the change detection algorithm described in the previous section. Two sets of data were collected³ at Fort Indiantown Gap (FITG), Pennsylvania, robotics research facility. Each set consisted of a base run, in which the UGV traversed a path through natural terrain, and several variant runs. The variant runs traversed the same terrain along a similar path, but in each variant, one or more intentional changes were introduced. Data sets from patrols were recorded and the change detection algorithm was applied off line. Detection of the intentional change was the goal of the exercise.

5. Results

The first data set was a deciduous wooded terrain in November, and the intentional change was the introduction of a person. Several variant runs were conducted, but the navigation system drifted between runs so that misalignment of the data between runs was as great as the intentional change.⁴ Of this set, only one variant was deemed sufficiently aligned to evaluate. The patrols of this data set are FITG 143 and FITG 144. With a naming convention, the comparison is named FITG 143-144.

The second data set was a dirt road between two scrubby deciduous tree lines in May. The base run is FITG 129, and the intentional change was the introduction of a person in one variant (FITG 130) and the introduction of a person and a small lunch box roughly a 0.2-meter cube (FITG 131). These runs were very well aligned.

³Thanks to Dr. Nicolas Vandapel and Dr. Martial Hebert, of Carnegie Mellon University, and the FITG staff of GDRS.

⁴In principle, the data could have been aligned, perhaps by a method such as iterative closest point, but the alignment was deemed beyond the scope of this study.

In neither data set was ground truth collected rigorously, but the person-size changes were evident in the raw data as visualized in a VRML viewer⁵ (see figure 2b). The location of the lunch box was known approximately, and it, too, was roughly visible in the source data.

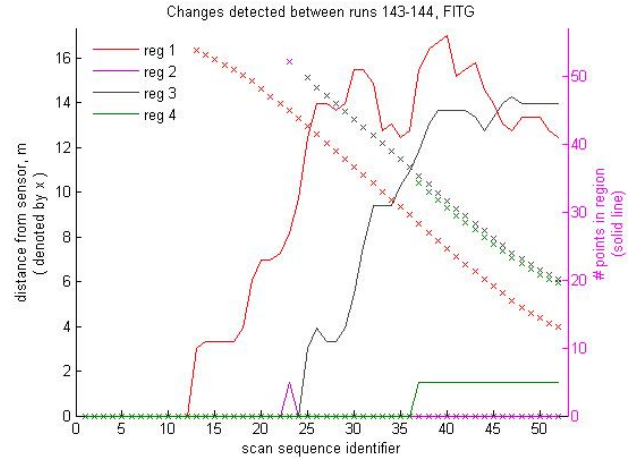
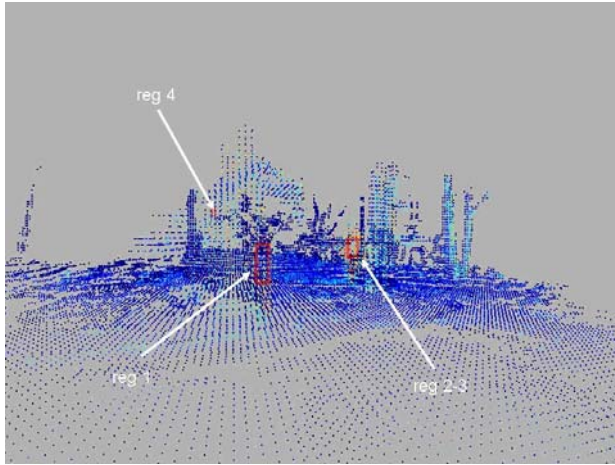
The primary measure of merit was the effectiveness of the algorithm in detecting the region of intentional change while not detecting change in other regions of the scene, assumed to be ephemeral noise. A second measure of interest is the distance at which a change region was detected and the persistence of the detection. To track this measure, change detection was evaluated at events scheduled at intervals of 30,000 data points (equivalent to approximately 0.5 second of data from the sensor) throughout processing of sensor data from the second patrol.⁶ At each scheduled event, change voxels were extracted from the volume and change regions assessed. Change regions were then matched to *persistent regions* from the previous evaluation event, again based on spatial proximity. The results were projected to a virtual image at the instantaneous vantage point of the vehicle, and false color corresponding to the degree of change assigned to each non-free-space voxel was assigned. Presented as a movie, the 3-D nature of the terrain is quite apparent, but for the purpose of this report, a static image must suffice. Change regions in the image were surrounded by red boxes. The distance from the sensor location to the change region centroid was computed and the number of change voxels comprising the change region recorded. At the end of evaluation of the second patrol, the trajectories of change region size and distance from the sensor were plotted.

5.1 FITG 143-144

In the virtual image of the difference between runs 143 and 144, red boxes representing two human-size targets can be seen among the trees, as well as a small red box in the tree branches. In the accompanying plot, the trail of red x's beginning at abscissa value 13, read from the left-hand ordinate axis, tells us that the first intentional human-size change (reg 1) is detected first at a range of 16 meters. The same color solid line, read from the right-hand ordinate axis, tells us that reg 1 initially contains 10 change points. Following the trail of red markers, we can see that reg 1 is tracked throughout the patrol, increasing in size (number of detected change voxels) as more sensor data become available. The second intentional human-size change (reg 2, in magenta) is detected at 16 meters' distance, lost momentarily, and reacquired at 15 meters as reg 3, in black. At 11 meters' distance, the small red box in the tree branches is acquired as reg 4 and tracked to the end of the patrol. There was no intentional change at this position, so the change must be considered a false positive (though it could have been a bird or squirrel unnoticed by the researchers).

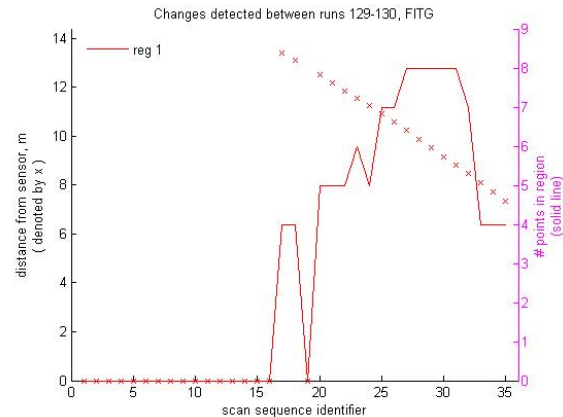
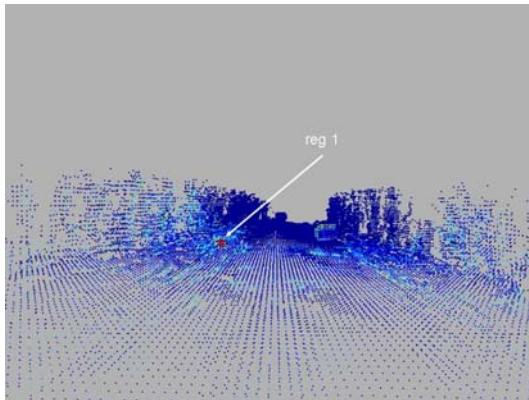
⁵VRML (Virtual Reality Modeling Language) is a standard file format for describing virtual 3-D worlds. Points collected by the ladar sensor were formatted for display by an interactive VRML viewer, allowing the 3-D structure of the data to be visualized.

⁶It would have been more intuitive to schedule the events at time-based intervals, but the time of acquisition was not available in the processed sensor data.



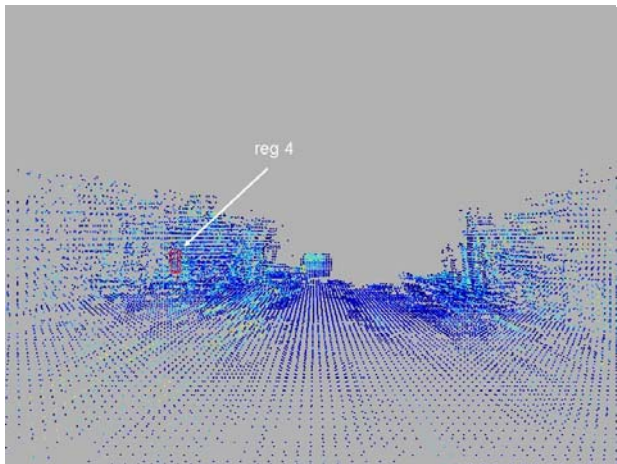
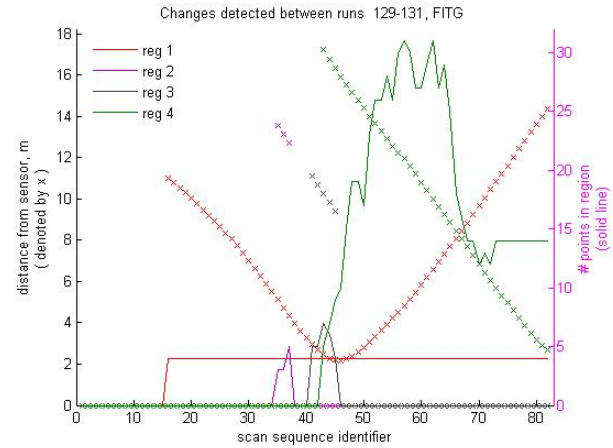
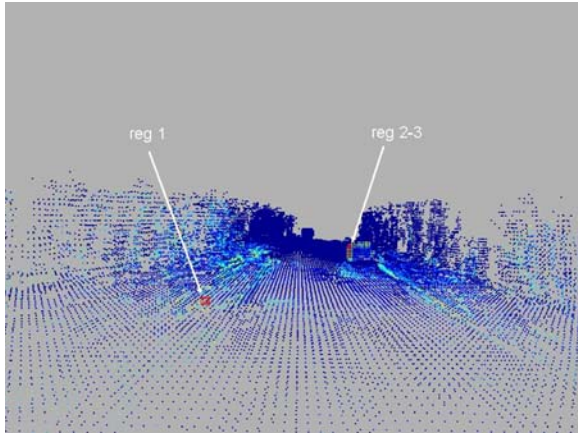
5.2 FITG 129-130

In the data set, a small lunch box was placed along the wooded dirt road. The small red box indicating a change region is apparent in the virtual image, and the graph indicates that the detection was made at a range of more than 13 meters. However, after the small item was tracked for roughly 6 meters, the change region diminished in size and disappeared since the algorithm concluded that, based on the accumulated evidence, there was not a change after all. (The patrol continued, although the plot ended with no change regions to report.) This represents a partial success since the change region detected should have persisted.



5.3 FITG 129-131

In this data set, the small lunch box (reg 1) was detected at a range of 11 meters and is depicted at the left of the upper virtual image. It was tracked successfully as a region of change of apparent size 4 voxels until the end of the patrol, although no new data were available past scan sequence 40 or thereabouts since the lunch box was no longer in the field of view of the sensor.



This sequence is represented by two virtual images since no single image contained all the detected change regions. The upper image corresponds to scan sequence (abscissa value) 35 and the lower image to scan sequence 75.

Also apparent in the upper virtual image is a small red box designated by the white arrow. This is reg 2, which is lost momentarily and reacquired as reg 3. This region is a false positive resulting from the effect of occlusion. The object causing the detection was viewed from the front and side during the traverse of patrol 129, but during the early portion of patrol 131, only the front could be seen. As the vehicle drew near, the side became increasingly visible and the difference in appearance fell below the change threshold, so the algorithm ceased to declare the voxels changed. It was identified as a false positive for 5 meters from the total patrol of ~40 meters, with a maximum apparent size of 7 voxels.

Visible in the lower virtual image is reg 4, a human-size region of intentional change. It is detected at a range of 17 meters and tracked successfully to the end of the patrol.

6. Discussion

6.1 Distribution of Voxelized Data

During ray tracing, when a ray encounters a voxel, it passes through the voxel (evidence that the voxel is unoccupied) or it terminates (evidence that the voxel is occupied by something). During a run, a voxel will likely be encountered by dozens to thousands of rays. $P(\text{occ})$ is a measure of the proportion of incident rays that are reflected, which is aggregated evidence of the likelihood that the voxel is occupied. Figure 3 plots p_1 at the end of the first patrol for one of the patrol pairs and is not dissimilar from plots for the others. Only those voxels with $P(\text{occ}) > 0.1$ are plotted; voxels encountered with $P(\text{occ}) < 0.1$ (clearly free-space voxels) are not shown. In the data sets of this study, clearly free-space voxels comprised about 80% of voxels encountered.

Although not apparent in the plots, it was noted that the voxels with intermediate values of $P(\text{occ})$ tended to cluster around voxels with high values of $P(\text{occ})$. This can be viewed as a spatial blurring of the voxel content over nearby voxels.

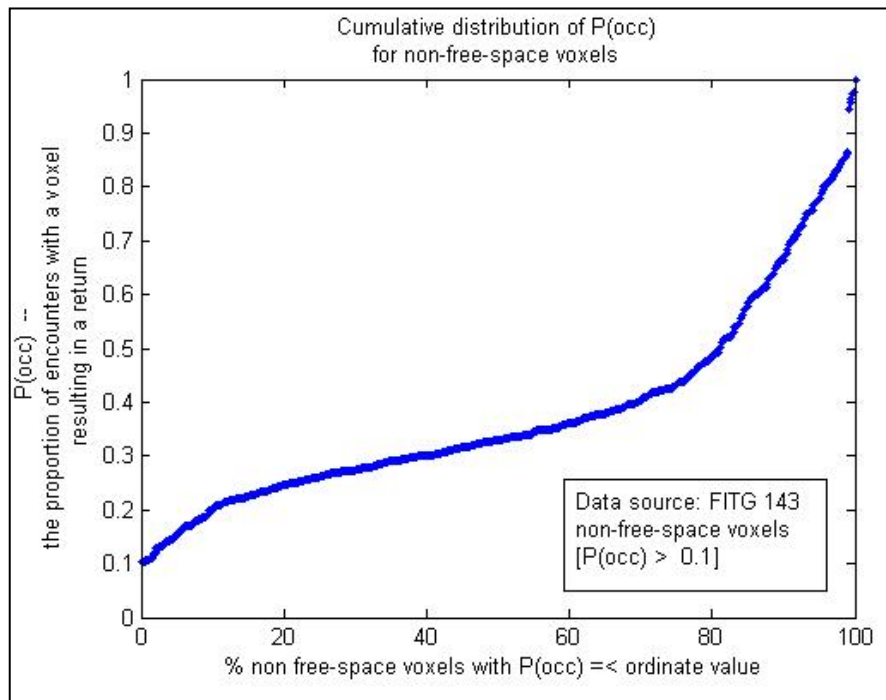


Figure 3. Cumulative distribution of p_1 for patrol 143.

The thing that makes change detection difficult is that the evidence grid method does not classify the volume clearly as occupied or unoccupied. Some of the effects that confuse the measure are now described.

6.2 Vantage Point

As the vehicle moves along its path, the terrain sampled by the sensor is determined by the vantage point of the sensor in full 6 degrees of freedom. The sampling is thus determined in part by the path of the vehicle through the scene, which is not tightly specified in the scenario. The aggregated sensor data are also affected by time derivatives of the vehicle path. If the vehicle travels more slowly, the terrain is sampled at a relatively higher spatial rates. In this study, the sensor was mounted on a pan/tilt device,⁷ adding to the complexity of the sampling.

6.3 Occlusion

Occlusion describes the obstruction of the line of sight to some object by some other, nearer object, resulting in the more distant object not being seen in its totality. The partially obstructed object is described as being *occluded* by the nearer object. In the context of this study, as the vehicle moves along its path, some features previously occluded may become visible, and vice versa, that is, the *appearance* of the scene changes.

6.4 Surface Versus Volume

Representing the data as XYZ data in a common reference frame, as required to integrate terrain information as the sensor moves, implicitly treats the world as a volume. However, the aggregated sensor data describe only a set of surfaces visible from the path described by the sensor, which is limited to observations in the instantaneous line of sight. Not only are some terrain features occluded by others, but elements of terrain features are self-occluded (for example, the far side of a tree trunk is occluded by the near side of the same trunk).

6.5 Range Effects

The volume swept by each rangefinder measurement is effectively in spherical coordinates, while the voxels into which the world model is subdivided are Cartesian. Voxels near the vehicle may be oversampled by a scan, while those farther away are undersampled. The lidar of this study samples at roughly 0.5-degree intervals in both horizontal and vertical directions, so a facet of a voxel corresponds to the cross section of the rangefinder at a range of approximately 12 meters.

In addition to effects that blur $P(\text{occ})$ of a voxel during a single patrol, two additional effects impact the difference **diff** between $P(\text{occ})$ for two different patrols.

6.6 Path Dependence

While the pairs of patrols traverse the same terrain, the path followed by the UGV in each patrol is not closely controlled and may diverge somewhat—in this study, by a couple of meters. The vantage point therefore changes not only within a patrol but between patrols as well.

⁷Motion of the pan/tilt device was instrumented. The effect of this motion was factored into the mapping of sensor points into the world coordinate system.

6.7 Registration

Since all sensor data in this scheme are converted to a common world coordinate system, it is important that the coordinate system be stable. The key element in maintaining the world coordinate system is the navigation system of the moving vehicle. Real-world navigation systems experience error that varies with time (*drift*), and in simple navigation systems, that error can become quite large. Sensor data assigned to the wrong voxel because the navigation system is in error will be compared to sensor data from a completely different terrain, potentially leading to nonsensical results. Errors in registration caused several data sets from this study to be discarded.

6.8 Distribution of the Difference in Voxel Content

Figure 4 plots the cumulative distribution of the **diff** attribute at the end of one of the patrol pairs. As in figure 3, voxels that were discovered to be clearly free space are not plotted. The value plotted represents the difference, on a voxel-by-voxel basis, between the P(occ) from the first patrol and the P(occ) from the (entire) second patrol. Since the terrain is assumed to change very little except for the intentional changes introduced, we expect the measures of P(occ) from the two patrols to be highly correlated and the measure of the difference between P(occ) for the same voxel to be small. Although changes can occur because of the changes described, a large change is unlikely unless there has truly been a change in the voxel content. The threshold **v_threshold** is set accordingly high. A value of 0.8 was found to be effective in selecting voxels of known change.

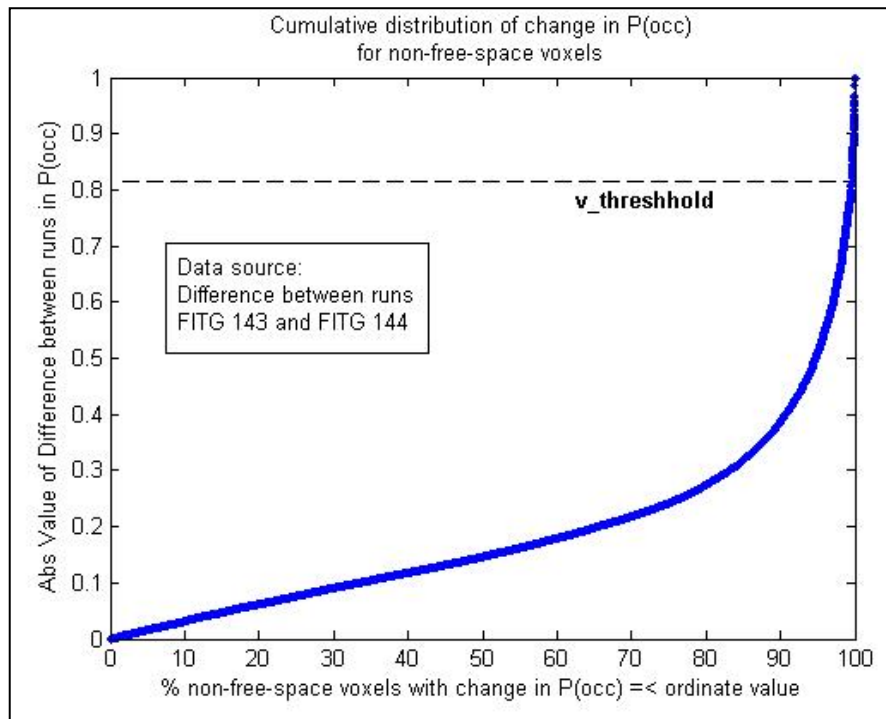


Figure 4. Cumulative distribution of **diff** between patrol 143 and 144. (Non-free-space voxels not plotted.)

7. Conclusions

This study was undertaken to establish a basis for detecting change in 3-D data from a moving imaging lidar. The three pairs of patrols described in this report are insufficient to draw any firm conclusions concerning the effectiveness of the approach in detecting changes between patrols. Further study of parameters used in voxelization, thresholding, and region growing would be required, as would more data from terrain differing in content and tools to correct errors in registration between patrols. The results achieved in the study show promise for restricted circumstances but seem unlikely to be useful in a real-world application.

As a precursor to the intended study of detecting moving objects (e.g., pedestrians) from a moving platform, however, the results indicate a promising direction. The approach used here, that is, operating on voxelized and normalized sensor data, rather than the raw data itself, is effective in identifying regions of change, at least in the circumstances of this study. The approach of tracing line segments (rays) emanating from the sensor position and terminating at the XYZ position of the return appears a useful counterpoint to the location of the return in defining an evidence-based measure of voxel content. These concepts can be carried over to an ensuing study. In addition, it is anticipated that the *ad hoc* approach implemented here can be improved if a more rigorous probabilistic framework is applied to the voxel measures and their evaluation.

8. References

- Amanatides, J.; Woo, A. A Fast Voxel Traversal Algorithm for Ray Tracing. In *Proceedings of Eurographics '87* **1987**, 3–10, G. Marechal, Ed. Elsevier North-Holland, New York.
- Bhanu, B., et al., eds. “Automatic Target Recognition” Special issue, *IEEE Transactions on Image Processing* 6, no.1 (Jan 1997).
- Juberts, M.; Barbera, A. Status Report on Next Generation Ladar for Driving Unmanned Ground Vehicles. In *Proceedings of SPIE Mobile Robots XVII* **2004**, 5609 , Bellingham, WA.
- Maintz, J.B.A.; Viergever, M.A. A Survey of Medical Image Registration. In *Medical Image Analysis* **1998**, 2, 1–36.
- Martin, M.; Moravec, H. *Robot Evidence Grids*, Robotics Institute; CMU-RI-TR-96-06; Carnegie Mellon University: Pittsburgh, PA, March 1996.
- Pacis, E. B.; Everett, H. R.; Farrington, N.; Kogut, G.; Sights, B.; Kramer, T.; Thompson, M.; Bruemmer, D.; Few, D. *Transitioning Unmanned Ground Vehicle Research Technologies*. DTIC ADA432516, 2005.
- Radke, R.; Srinivas, A.; Al-Kofahi, O.; Roysam, B. Image Change Detection Algorithms: A Systematic Survey. In *IEEE Transactions on Image Processing*, **March 2005**, 14(3), 294–307.
- Schutz, C.; Hugli, H. Change Detection in Range Imaging for 3D Scene Segmentation. In *Proceedings of SPIE Vision Systems: Applications* **1996**, 2786, 98-106, Besancon, France.
- Shneier, M.; Chang, T.; Hong, T.; Cheok, G.; Scott, H. A Repository of Sensor Data for Autonomous Driving Research. In *Proceedings of the SPIE Aerosense Conference* **2003**, 390-395, Orlando, FL.
- Tuong Thuy Vu; Matsuoka, M.; Yamazaki, F. LIDAR-Based Change Detection of Buildings in Dense Urban Areas. In *Proceedings of Geoscience and Remote Sensing Symposium* **2004**, 5, 3413–3416.

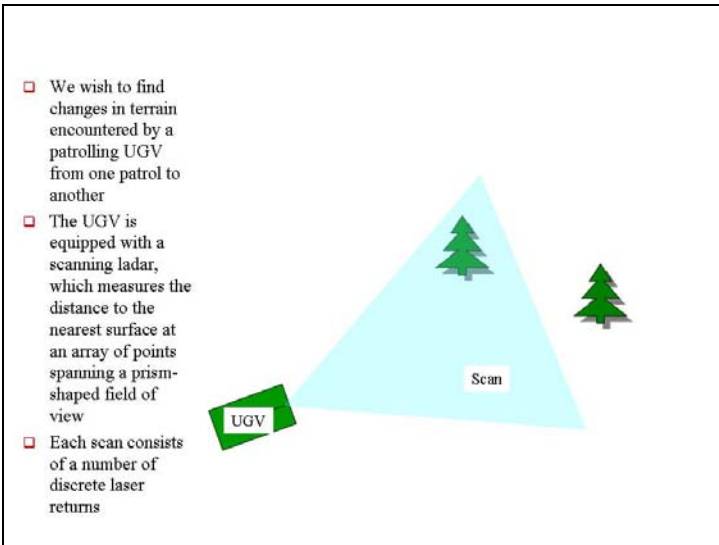


Figure A-1. Objective: Find change from patrol to patrol.

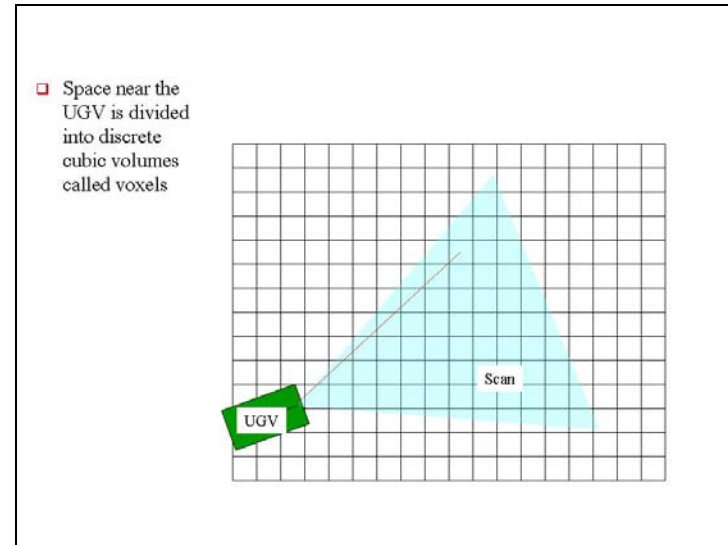


Figure A-3. Space interpreted as voxels.

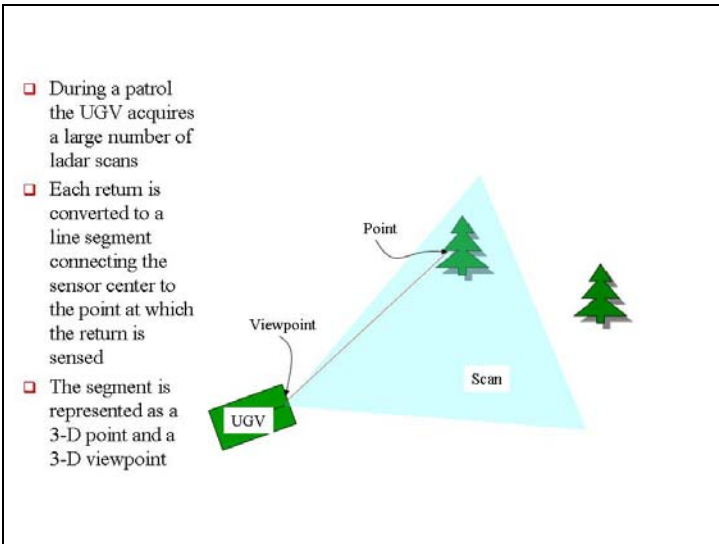


Figure A-2. Lidar return interpreted as line segment.

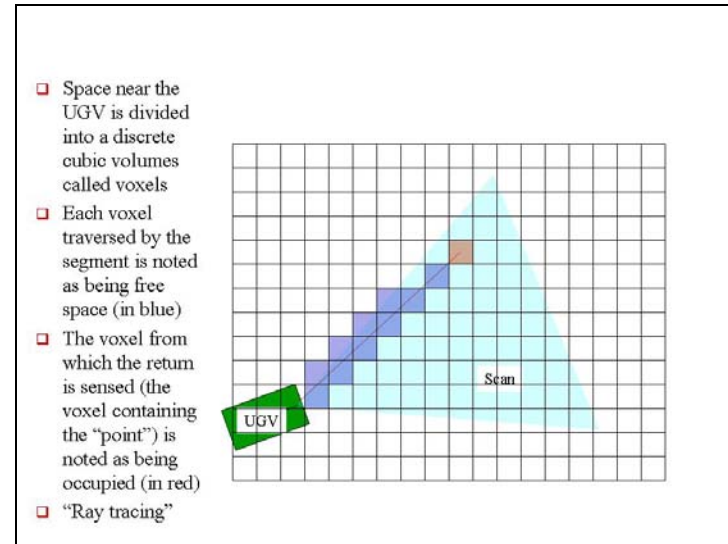


Figure A-4. Tracing a "ray".

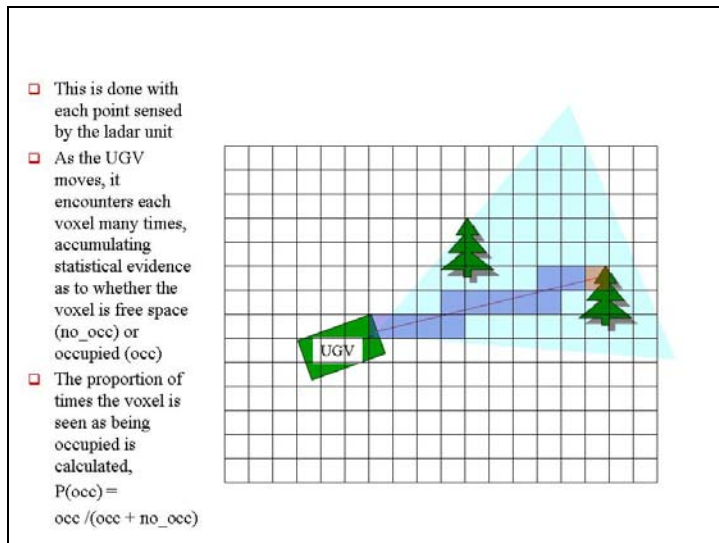
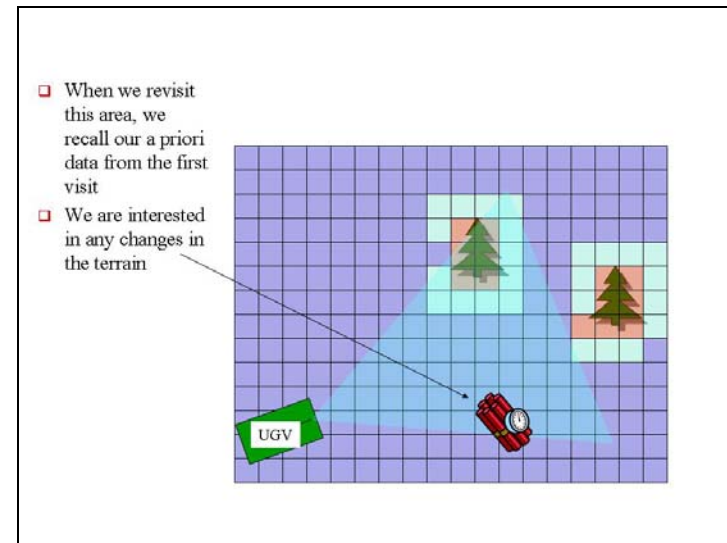
Figure A-5. Probability that a voxel is occupied, $P(\text{occ})$ 

Figure A-7. Ready for second patrol

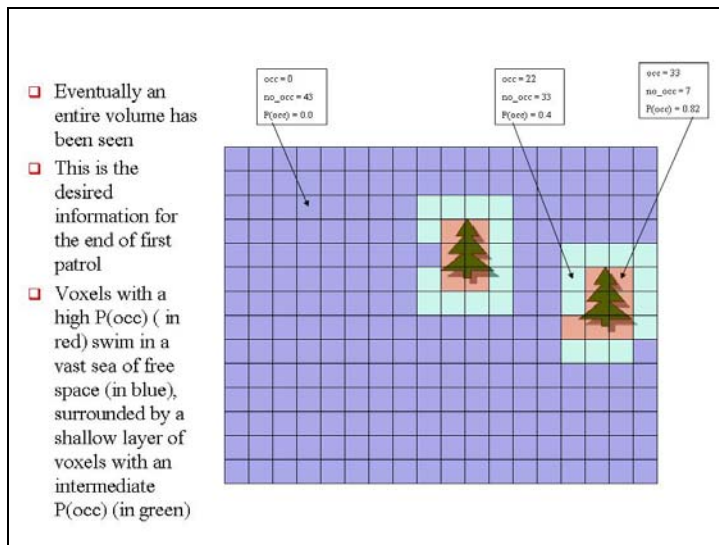


Figure A-6. Voxel state at end of first patrol

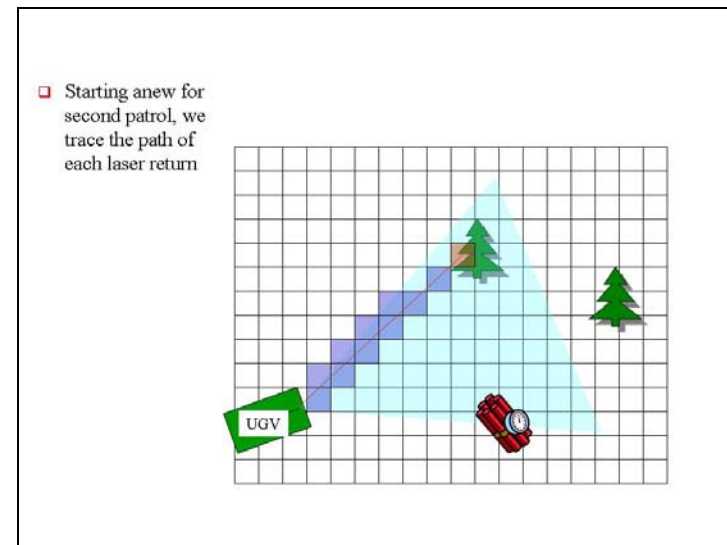


Figure A-8. Begin second patrol

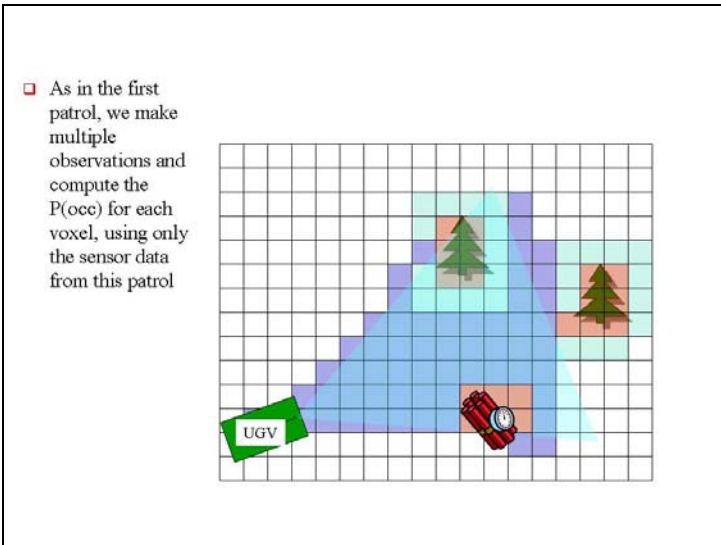


Figure A-9. Find $P(occ)$ for each voxel during second patrol

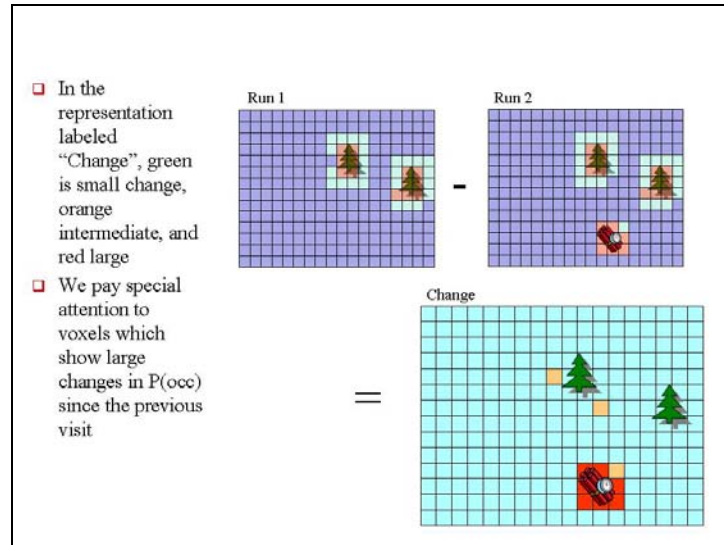


Figure A-11. Find change voxels

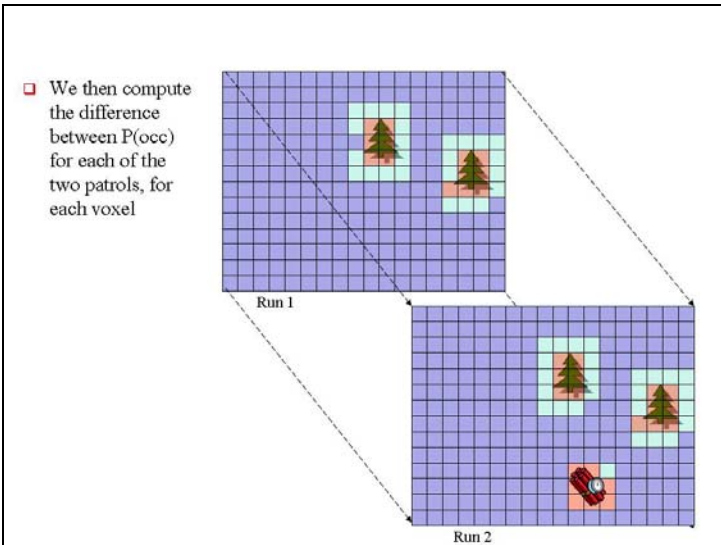


Figure A-10. Compare $P(occ)$ for the two patrols

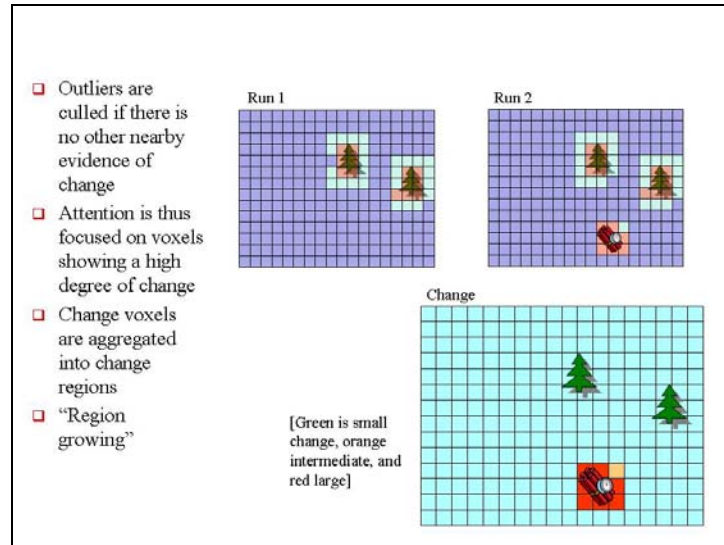


Figure A-12. Find change regions

<u>NO. OF COPIES</u>	<u>ORGANIZATION</u>
1 (PDF ONLY)	DEFENSE TECHNICAL INFORMATION CTR DTIC OCA 8725 JOHN J KINGMAN RD STE 0944 FORT BELVOIR VA 22060-6218
1	US ARMY RSRCH DEV & ENGRG CMD SYSTEMS OF SYSTEMS INTEGRATION AMSRD SS T 6000 6TH ST STE 100 FORT BELVOIR VA 22060-5608
1	DIRECTOR US ARMY RESEARCH LAB IMNE ALC IMS 2800 POWDER MILL RD ADELPHI MD 20783-1197
1	DIRECTOR US ARMY RESEARCH LAB AMSRD ARL CI OK TL 2800 POWDER MILL RD ADELPHI MD 20783-1197
2	DIRECTOR US ARMY RESEARCH LAB AMSRD ARL CS OK T 2800 POWDER MILL RD ADELPHI MD 20783-1197
2	DIRECTOR US ARMY RESEARCH LAB AMSRD ARL CI CB B O'BRIEN S YOUNG 2800 POWDER MILL RD ADELPHI MD 20783-1197
1	DIRECTOR US ARMY RESEARCH LAB AMSRD ARL SE RU B STANTON 2800 POWDER MILL RD ADELPHI MD 20783-1197
1	NATL INST OF STDS & TECHNOLOGY ATTN DR J ALBUS BLDG 200 GAITHERSBURG MD 20899
1	CARNEGIE MELLON UNIV ROBOTICS INST DR M HEBERT 5000 FORBES AVE PITTSBURGH PA 15213

<u>NO. OF COPIES</u>	<u>ORGANIZATION</u>
1	UNIV OF MARYLAND INST FOR ADV COMPUTER STUDIES ATTN DR L DAVIS COLLEGE PARK MD 20742-3251
3	US ARMY TARDEC ATTN AMSRD TAR R MS 205 B BRENDL MS 264 D THOMAS J JACZKOWSKI WARREN MI 48397-5000
1	US ARMY RS JPO ATTN SFAE GCS UGV E M WHITTIER REDSTONE ARSENAL AL 35898
1	DIR OF COMBAT DEVELOPMENT ATTN ATZK FD W MEINSHAUSEN BLDG 1002 ROOM 326 1ST CAVALRY DIV RD FT KNOX KY 40121 9142
1	CDR ARMY RSCH OFC ATTN R ZACHERY 4300 S MIAMI BLVD RSCH TRIANGLE PK NC 27709
1	SRI INTERNATIONAL ATTN DR K KONOLIGE 333 RAVENSWOOD AVE MENLO PARK CA 94025-3493
1	UNIV OF PENNSYLVANIA DEPT OF MECH ENGNRG ATTN DR V J KUMAR 229C TOWNE BLDG 220 SOUTH 33RD ST PHILADELPHIA PA 19104-6315
1	SAIC ATTN SCOTT FISH 8303 N MOPAC EXPWY STE B450 AUSTIN TX 78759
1	SANDIA NATL LABS ATTN J FEDDEMA MGR INTEL SYS CONTROLS DEPT 06634 PO BOX 5800 MS 1003 ALBUQUERQUE NM 87185
1	AFRL/MLQF ROBOTICS RSCH GROUP ATTN BRIAN SKIBBA 104 RESEARCH RD BLDG 9738 TYNDALL AFB FL 32403

<u>NO. OF</u> <u>COPIES</u>	<u>ORGANIZATION</u>
1	CDR AATD ATTN AMSRD AMR AA I K ARTHUR LEE BLVD BLDG 401 FORT EUSTIS VA 23604-5577
1	US ARMY CERDED NVESD ATTN AMSRD CER NV GCSD (KLAGER) 10221 BURBECK ROAD FORT BELVOIR VA 22060-5806
2	GENL DYNAMICS ROBOTIC SYS ATTN M DELGIORNO K BONNER 1234 TECH CT WESTMINSTER MD 21167-3029
2	ROBOTICS RESEARCH ATTN C SHOEMAKER K MURPHY A LACAZE 814 W DIAMOND AVE STE 301 GAITHERSBURG MD 20878
2	SPAWAR SYSTEMS CTR CODE 2371 C HUDSON B EVERETT 53560 HULL ST SAN DIEGO CA 92152-5001
2	DARPA/IPTO ATTN DR L JACKEL D NEWMAN 3701 N FAIRFAX DR ARLINGTON VA 22203
<u>ABERDEEN PROVING GROUND</u>	
1	DIRECTOR US ARMY RSCH LABORATORY ATTN AMSRD ARL CI OK (TECH LIB) BLDG 4600
1	US ARMY AMSAA ATTN AMSRD AMS SC J PUSEY BLDG 392
2	DIRECTOR US ARMY RSCH LABORATORY ATTN AMSRD ARL WM J SMITH P BAKER BLDG 4600
2	DIRECTOR US ARMY RSCH LABORATORY ATTN AMSRD ARL WM B M ZOLTOSKI J MORRIS BLDG 4600

<u>NO. OF</u> <u>COPIES</u>	<u>ORGANIZATION</u>
7	DIRECTOR US ARMY RSCH LABORATORY ATTN AMSRD ARL WM BF H EDGE S WILKERSON M FIELDS J SHUMAKER R VONWAHLDE G HAAS (2 CYS) BLDG 390
1	DIRECTOR US ARMY RSCH LABORATORY ATTN AMSRD ARL WM RP J BORNSTEIN BLDG 1121
1	DIRECTOR US ARMY RSCH LABORATORY ATTN AMSRD ARL HR SE T KELLEY BLDG 459